

This is an Open Access document downloaded from ORCA, Cardiff University's institutional repository: <https://orca.cardiff.ac.uk/id/eprint/102592/>

This is the author's version of a work that was submitted to / accepted for publication.

Citation for final published version:

Nguyen, Hong K. D., Sankar, Gopinathan and Catlow, Charles Richard A. 2016. Effects of the synthetic condition on the stability, particle size and redox chemistry of nanoporous CoAlPO-34. *Journal of Porous Materials* 24 (3) , pp. 567-572.  
10.1007/s10934-016-0292-y

Publishers page: <http://dx.doi.org/10.1007/s10934-016-0292-y>

Please note:

Changes made as a result of publishing processes such as copy-editing, formatting and page numbers may not be reflected in this version. For the definitive version of this publication, please refer to the published source. You are advised to consult the publisher's version if you wish to cite this paper.

This version is being made available in accordance with publisher policies. See <http://orca.cf.ac.uk/policies.html> for usage policies. Copyright and moral rights for publications made available in ORCA are retained by the copyright holders.



# Effects of the synthetic condition on the stability, particle size and redox chemistry of nanoporous CoAlPO-34

Hong K. D. Nguyen<sup>1</sup> · Gopinathan Sankar<sup>2</sup> · Richard A. Catlow<sup>3</sup>

**Abstract** This study focuses on the effect of the synthetic conditions on the stability, particle size, redox chemistry of cobalt into the framework of CoAlPO-34. It seems that the most sufficient pH for the substitution of Co into the framework of CoAlPO-34 was pH around 7.5 when the as-synthesized bifunctional catalyst has the best redox property. The pH of the initial gel has strong effect on the particle size of CoAlPO-34. The substitution of cobalt and redox chemistry were determined by: EXAFS combined with XRD, XANES, IR. Stability of the nanoporous catalyst studied by in situ XRD were also reported.

**Keywords** Aluminophosphates CoAlPO-34 Gel pH Bifunctional catalyst Nanoporous

## 1 Introduction

Since the discovery of nanoporous aluminophosphates, special interest is devoted to chabazite-type structures.

With small pore size of 3.8 Å, these molecular sieves display interesting catalytic activities of organic reactions involving small molecules. In the MTO process [1],

aluminophosphate chabazite gives a narrow product distribution with a high selectivity to C<sub>2</sub>–C<sub>4</sub> olefins [2, 3]. Besides MTO process, these catalysts can also exhibit high shape selectivities allowing the diffusion of only small or linear molecules [4].

Many efforts have been made to improve selectivity towards the desired product, by various physico-chemical modifications of small pore materials. For example, ethylene selectivity (from dehydration of methanol) can be improved by incorporating transition metals such as Co, Mn, and Ni into the framework of AlPO-34 and SAPO-34 [5]. CoAlPO-34 catalysts also show exceptionally high performances in the oxidation of NO to NO<sub>2</sub>, and poor activity in other DeNO<sub>x</sub> reactions [6, 7]. The incorporation of transition metal ions to the framework sites is of particular interest since the incorporated paramagnetic metal species can generate catalytically reactive sites rendering MeAlPO materials potentially useful catalysts. Accordingly, information on the redox chemistry and the particle size of the introduced metal ions in the aluminophosphate framework is also of special interest.

The transition metal focused on within this work was cobalt. Compared to other first row transition metals, which usually prefer octahedral coordination geometry, Co<sup>2+</sup> preferably adopts tetrahedral stereochemistry with oxide ions as ligands. Different from other reported paper, this study focuses on the effect of the synthesis conditions (pH of initial gel, temperature) on the stability, particle size, redox chemistry and the substitution of Cobalt into the framework of CoAlPO-34 to identify ways of producing high surface area, thermally stable materials, with well defined micropores and suitable distributions of catalytically active sites.

---

& Hong K. D. Nguyen  
dieuhong\_bk@yahoo.com

<sup>1</sup> School of Chemical Engineering, C4-306, Ha Noi University of Science and Technology, No 1 Dai Co Viet Road, Ha Noi, Viet Nam

<sup>2</sup> Department of Chemistry, University College London, 20 Gordon Street, London WC1H 0AJ, UK

<sup>3</sup> Head of MAPS Faculty, Department of Chemistry, University College London, 20 Gordon Street, London WC1H 0AJ, UK

## 2 Experimental

### 2.1 Synthesis of CoAlPO-34

Samples were synthesized with different experimental conditions using  $\text{Al}(\text{OH})_3$ , phosphoric acid 85 %, distilled water,  $\text{Co}(\text{Acetate}) \cdot 2\text{H}_2\text{O}$  and TEAOH. After the synthesis, the crystals were filtered, washed with distilled water and dried. Typical gel composition for CoAlPO-34 was  $0.9\text{Al}:(0.9-1.5)\text{P}:0.1\text{Co}:(0.8-1.2)\text{TEAOH}:25\text{H}_2\text{O}$ .

### 2.2 Characterization procedure

The samples first will be characterized by XRD collected at room temperature using a Siemens D500 diffractometer using Cu K radiation ( $\lambda = 1.5418 \text{ \AA}$ ) at room temperature to determine the structure and investigate the phase's purity. The samples then were deeper characterized by in situ combined EXAFS/XRD. Crystal size, shape and chemical analysis of catalysts were obtained by a cluster of three Scanning Electron Microscopes at Institute of Archaeology, UCL, London. XANES examinations reported in this paper were all recorded at station BM26-ESRF, Grenoble-France. Combined XRD/EXAFS were collected to investigate the stability of the material during the calcination process.

## 3 Results and discussion

### 3.1 Effect of the synthetic conditions on the particle size of nanoporous CoAlPO-34

The synthetic conditions and composition of the initial gel are summarized in Table 1. XRD of as-synthesized CoAlPO-34 samples were shown in Fig. 1. It can be seen that XRD patterns of all products showed the materials to be phase pure, related to chabazite structure. However, the XRD of sample synthesized at pH 6.0 have some additional

Table 1 Synthetic conditions for the crystallization of CoAlPO-34

$\text{pH}_{\text{initial}}$	Compositions Al:P:Co:Template:H <sub>2</sub> O	Temperature (LC)	Time (h)
Synthetic conditions			
6.0	0.90:1.50:0.10:0.80:25	150	15
6.5	0.90:1.30:0.10:0.80:25	150	15
7.0	0.90:1.20:0.10:0.80:25	150	15
7.5	0.90:1.10:0.10:0.80:25	150	15
8.0	0.90:1.00:0.10:1.00:25	150	15
8.5	0.90:1.00:0.10:1.20:25	150	15

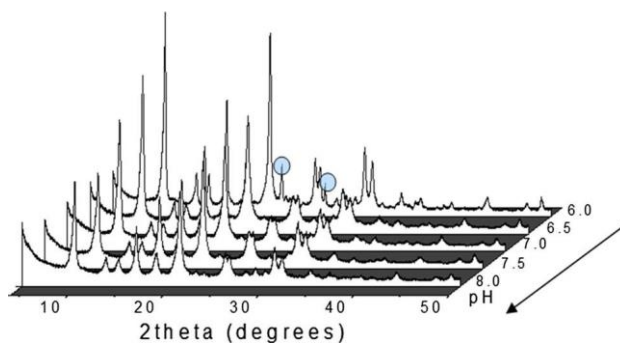


Fig. 1 XRD patterns of as-synthesized CoAlPO-34 with different pH of the initial gel

peaks at around  $2\theta = 21$  and  $27$  corresponds to the dense tridymite type  $\text{AlPO}_4$  phase [8]. Although it appears that a fraction of the material is transformed to tridymite dense phase, majority of the sample crystallized at pH 6.0 still possess the CHA structure and the XRD shows all the typical peaks with good intensity suggesting that both tridymite and CHA phase co-exist under these preparation conditions.

Chemical compositions obtained by EDX of as-synthesized samples are given in Table 2.

As it is present in the starting gel, cobalt is expected to substitute exclusively for aluminium. So after the synthesis, the ratio of P should be equal the molar ratio of total amount (Al + Co).

As seen from the gel's initial composition (Table 1), the P amount is slightly higher than Al + Co, i.e. [1.0 molar ratio]. The reason for that is that P was used to control the pH. The expected amount of P to be related to Al is still 1.0 molar ratio. So it can be said that the composition given in the table above summarize the degree of cobalt in the crystal phase (at framework or extra-framework position). In fact there may be Co species incorporated in the framework as well as at extra framework positions (trapped in cages or in amorphous phases), shown as a whole in chemical composition that can not be distinguished. In addition the error involved in these measurements may also contribute to the variation seen in the expected composition.

Table 2 Compositions in molar of as-synthesized CoAlPO-34s obtained by EDX

pH	Compositions, molar (O:P:Al:Co)
6.0	2.41:1.00:0.69:0.11
7.0	4.16:1.00:0.80:0.11
7.5	3.23:1.00:0.78:0.17
8.0	3.82:1.00:1.21:0.19
8.5	2.56:1.00:0.85:0.19

Figure 2 shows SEM images of as-synthesised CoAlPO-34. In general, SEM showed the as-synthesized samples to be composed of crystals with various diameter.

However, it can be observed from SEM that in the crystal phase of samples synthesized at pH 6.0 and 8.5, two different crystal sizes can be distinguished: crystals with size around 100–200nm and few bigger cubic crystals are observed with size 300–400nm.

From SEM it can be seen that, in general, the higher pH of the initial gel, the smaller the particle size. All the samples were synthesized under the same conditions except pH, so it is likely that pH affects the size and morphology of the crystal.

The reason for this observation is related to the nuclei formed during the crystallization in the gel. As reported, if

stabilized in the gel, the tetrahedral aluminum atoms which are unstable at low pH values will facilitate nanoporous phase formation [9, 10]. It has been shown that tetrahedrally coordinated aluminum originating from the depolymerization of aluminum hydroxide is stable in a gel containing amine [9]. It is proposed that the amine molecules are bound via the phosphate tetrahedra to the initial species consisting of  $AlO_4$  and  $PO_4$  tetrahedra [9].

This arrangement provides a hydrophobic environment around the active species, protecting them from the attack of water molecules and thus stabilizing the tetrahedral coordination of Al atoms. Thus, the higher pH may enhance the rate of depolymerization of aluminum hydroxide, which in the presence of a stoichiometric amount of phosphoric acid and templating amine

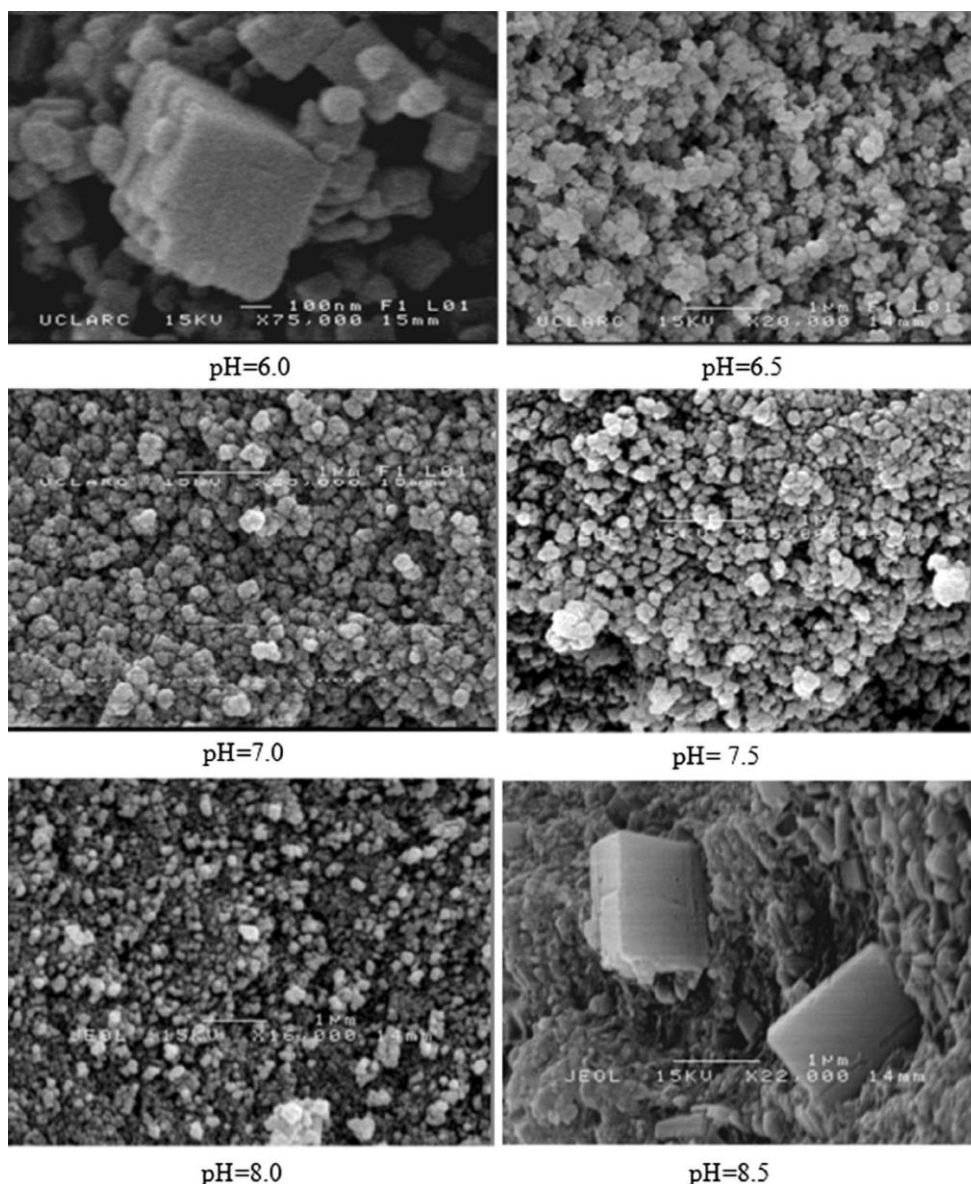


Fig. 2 SEM images of CoAlPO<sub>34</sub>s synthesized from initial gels with pH 6.0–8.5, at 150 LC in 15 h

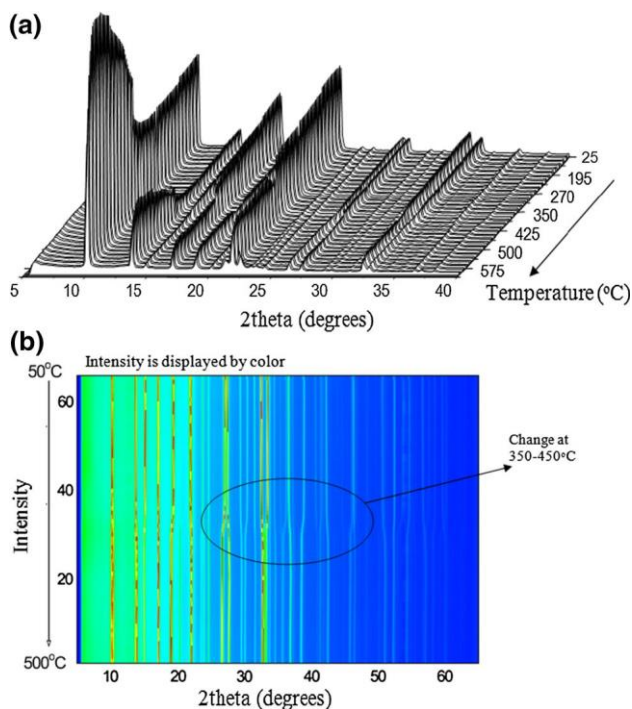


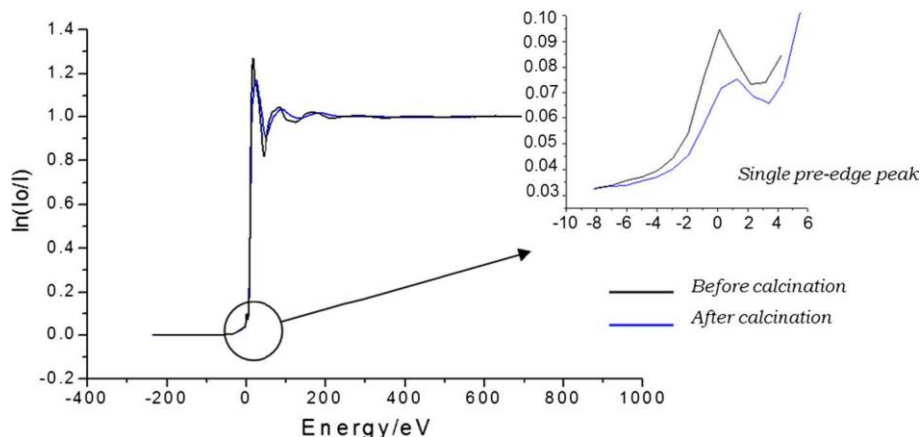
Fig. 3 Typical stacked XRD data recorded during calcination of CoAlPO-34 in a 3D plot; b 2D plot

molecules will stabilize the tetrahedrally coordinated Al species in the gel. Moreover, the higher pH was controlled by the increasing amount of template. For this reason, increasing pH means creating more nuclei formed in the gel for the crystallization, thus smaller particles were formed.

### 3.2 Effect of the synthetic conditions on the structural stability of nanoporous CoAlPO-34

The stability of AlPO-34 with CHA framework can be assessed from a plot of the XRD, recorded during the calcination process, as a function of temperature.

Fig. 4 Normalized XAS of sample synthesized at pH 7.5 before and after calcination up to 550 LC



Data shown in Fig. 3 was recorded on the HOTWAX detector (which is scientifically driven by Professor G. Sankar at the Royal Institution of Great Britain and Dr J. P. A. Fairclough at the University of Sheffield and in collaboration with detector group at RAL and Daresbury Laboratory). The 3D plot of the XRD data of CoAlPO-34 (Fig. 3a) reveals that the material is stable upon removal of the template molecule; there was no evidence of the framework collapsing on removal of the template, or loss of crystallinity in this process up to 580 LC.

As shown clearly from 2D-plot (Fig. 3b), the XRD intensity changes between 350 and 400 LC which is primarily due to the collapse of the structure directing organic template that occludes the pores of the microporous system. This is consistent with other studies that demonstrated that the organic template collapsed above 350 LC [7, 11].

The experiment was then repeated but with the heating profile increased to 650 LC. Our study shows that the nanoporous structure of the CoAlPO-34 materials synthesised in this work begin to lose its integrity above 600 LC and suggest that the catalysis should be performed below 600 LC.

### 3.3 Effect of the synthetic condition on the redox chemistry of nanoporous CoAlPO-34 by EXAFS

The substitution, the oxidation state and coordination environment of cobalt in the framework of as-synthesized CoAlPO-34 was investigated by EXAFS during calcinations. After the calcinations up to 550 LC, the colour of the samples changed from blue to different green shades: dark green, light or yellow green.

In many papers and reports [1, 7, 11, 12], EXAFS investigation strongly support that the oxidation of transition metal in general and  $\text{Co}^{2?}$  to  $\text{Co}^{3?}$  occurred upon the calcinations. Only the first shell Co-O was studied in this work, since the primary aim of the study is to understand the local environment around the central atom cobalt and

Table 3 The fraction of oxidized Co(III) in as-synthesized CoAlPO-34 samples upon calcinations up to 530 LC

pH of the initial gel	Fraction (%)
6.5	56
7.0	68
7.5	82
8.5	60

relate them to oxidation state. The shape of the K-edge and the pre-edge are characteristic for the local symmetry of the investigated atom and can be used as fingerprints in the identification of its local structure [11]. Co K-edge XAS spectra of as-synthesized CoAlPO-34 (Fig. 4) exhibits the characteristic tetrahedral pre-edge resonance, demonstrating that cobalt cations are incorporated into the tetrahedral sites. In XAS spectra of the calcined sample, the pre-edge peak is strongly diminished, indicating that in the process of calcination, the tetrahedral environment of the metal is distorted [1].

Sankar et al. [1] have reported that from the bond distance, it is possible to calculate the fraction of oxidized Co(III) after calcinations procedure, using the Vegard relationship. The fraction of oxidized Co(III) in as-synthesized CoAlPO-34s upon calcinations was calculated using this relationship and shown in Table 3.

The change in cobalt coordination number  $N$ , the average Co–O bond distance  $R$ , and the Debye–Waller factor  $A$  as a function of temperature for as-synthesized CoAlPO-34 samples are shown in Fig. 5a, b, c.

As shown in Fig. 5a, the best fit bond distance Co–O obtained for the first shell is 2.05 for the sample synthesized at pH 8.5. This value is much larger than those usually reported for CoAlPO<sub>4-n</sub> materials [1, 13–16], which are generally between 1.92–1.95 Å. This may indicate the presence of the Co<sup>2+</sup> octahedral species in the sample with the Co–O bond distance around 2.10 Å for a typical octahedrally coordinated system, which may lead to the rise of average Co–O bond distance. This result agreed with the changing colour observed for this sample to grey-black after the calcinations.

#### 4 Conclusion

It can be seen from the characterization of synthesized cobalt-substituted AlPO-34 that the synthetic conditions, especially pH of the initial gel has obvious effects on the morphology of samples, substitution of cobalt into the framework, the redox chemistry and the crystal size. The best pH for the substitution of cobalt into the framework of AlPO-34 is 7.5, that produces the highest fraction of

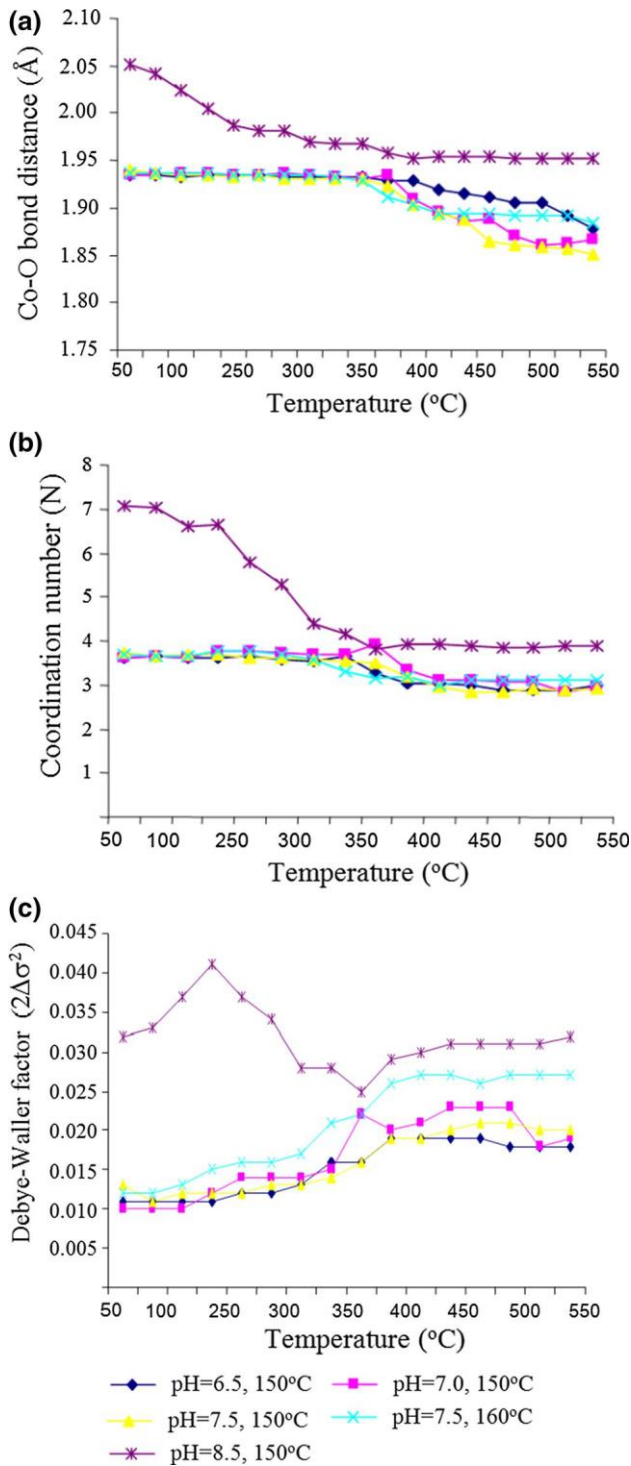


Fig. 5 Changes of a Co–O bond distance, b coordination number  $N$ , c the Debye–Waller factor  $A$  ( $2\Delta\sigma^2$ ) in CoAlPO-34 samples upon calcinations

oxidized cobalt, over 80 %. This is a high level compared with other reported materials such as CoAlPO-11, CoAlPO-36 and similar to the one observed for CoAlPO-18 and CoAlPO-34 reported previously [1, 5, 11, 16].

Acknowledgments This work was financially supported by the National Foundation for Science and Technology Development, Vietnam (NAFOSTED) under Grant Number 104.05-2013.57.

## References

1. G. Sankar, J.K. Wyles, C.R.A. Catlow, *Top. Catal.* 24(1–4), 173 (2003)
2. R.D. Delphine, L.O. Danile et al., *Fuel Process. Technol.* 83, 203 (2003)
3. E. Dumitriu, A. Azzouz, H. Asile et al., *Microporous Mater.* 10, 1 (1997)
4. J.M. Thomas, R. Raja, G. Sankar, R.G. Bell, *Acc. Chem. Res.* 34, 191 (2001)
5. M. Stöcker, *Microporous Mesoporous Mater.* 29(1–2), 3 (1999)
6. A. Frache, B.I. Palella, M. Cadoni, R. Pirone, H.O. Pastore, L. Marchese, *Top. Catal.* 22(1–2), 53 (2003)
7. G. Sankar, J.M. Thomas, J. Chen, P.A. Wright, P.A. Barrett, G.N. Greaves, C.R.A. Catlow, *Nucl Instrum Methods Phys Res B* 97, 37 (1995)
8. N. Raji, *J. Serb. Chem. Soc.* 70–3, 371 (2005)
9. B.L. Newalkar, B.V. Kamath, R.V. Jasra, S.G.T. Bhat, *Zeolites* 18, 286 (1997)
10. C.M. Chen, J.M. Jehng, *Catal. Lett.* 85(1–2), 73 (2003)
11. Hong K.D. Nguyen, G. Sankar, C.R.A. Catlow, *J. Porous Mater.* (2016). doi:10.1007/s10934-016-0275-z
12. Hong K.D. Nguyen, G. Sankar, C.R.A. Catlow, *Catal. Commun.* 25, 125 (2012)
13. K.J. Chao, A.C. Wei, H.C. Wu, J.F. Lee, Characterization of metal-incorporated molecular sieves. *Catal. Today* 49, 277 (1999)
14. S.H. Jung et al., *Microporous Mesoporous Mater.* 85, 147 (2005)
15. G. Sankar, R. Raja, in *Nanostructured Catalysts*, chap. 8, ed. by S. Scott et al. (Kluwer, 2003)
16. N. Rajic, A. Ristic, A. Tuel, V. Kaucic, A CoAPO-34 derived from a triclinic precursor prepared in the presence of HF. *Zeolites* 18, 115 (1997)